ORIGINAL PAPER

Windowing petrogenesis of continental flood basalts through mineralogical investigations: a case study from the Eastern Deccan Volcanic Province

Payel Dey[1] · Jyotisankar Ray[1] · Janisar M. Sheikh[2] · Suresh C. Patel[2] · Christian Koeberl[3,4]

Abstract

Evaluation of the petrogenetic history of continental flood basalt using mineral–chemical data has been sparingly used for several flood basalt provinces of the world. For the Deccan flood basalts, such attempts are still rudimentary. The present contribution highlights several facets of petrogenesis of the Eastern Deccan Volcanic Province using details of constituent phases including glass. The present-study area around Khandwa (21°49′N, 76°21′E) indicates the presence of three distinct lava flows, which were identified on the basis of physical volcanological features based on a three-tier classification. Moreover, the occasional presence of chilled dykes and feeder dykes has been documented. The lava succession rests above (apparent) cumulate gabbro basement. The lava flows, in general, are characterized by dominant pyroxene (mostly augite, locally pigeonite) and plagioclase, opaque (magnetite and ilmenite) and glass, whereas olivine is rare. Both of these principal mineral phases (namely, plagioclase and pyroxene) occur both as phenocrysts and groundmass, while opaque phases occur only as groundmass. Pyroxene and plagioclase are generally zoned due to the changing milieu of crystallization conditions. Pyroxene thermometry data show the equilibration temperature range of 1050–1300 °C. Except for two samples of Flow II and one sample of chilled zone, the pyroxene thermometry data are broadly similar to that obtained from magnetite–ilmenite thermometry. As expected, deduced glass thermometric data reveal a relatively higher temperature. Crystallization history of parental magma was quantitatively modeled using Petrolog 3 software. The results indicate that the parental magma underwent both equilibrium and fractional crystallization (for example initially crystallized olivine reacted with ambient liquid to give rise to pyroxene). Phenocrystal and groundmass plagioclase and pyroxene show distinct patterns of compositional zoning corresponding to fluctuating physical parameters within the magma. Some of the glass [especially from the chilled dyke, feeder dyke, and Upper Colonnade Zone (UCZ) of flow II and flow III] represents 'higher magnitude pressure ambience' (fossilized glass) which is distinct from 'surficial glass' caused by equilibrium quenching. The glass and pyroxene compositions (using tectonic discrimination diagrams) suggest a non-orogenic continental setting of the parent magma. It is concluded that the studied Deccan volcanism shows a complex interplay of repeated pulses of magma ascent, fluctuation of crystallization condition, effervescence, and local magma mixing.

Keywords Continental flood basalt · Eastern deccan volcanic province · Physical–volcanological features · Thermometer · Pyroxene quadrilateral · Continental tectonic setting · Oxygen fugacity

✉ Jyotisankar Ray
jsray65@hotmail.com

1 Department of Geology, University of Calcutta, 35, B. C. Road, Kolkata 700 019, India

2 Department of Earth Sciences, Indian Institute of Technology Bombay, Powai, Mumbai 400 076, India

3 Department of Lithospheric Research, University of Vienna, Althanstrasse 14, 1090 Vienna, Austria

4 Natural History Museum, Burgring 7, 1010 Vienna, Austria

Introduction

In Large Igneous Provinces (LIP), mineral composition often provides insight into the changing nature of the parental basalt magma system (Moore et al. 2018). This has been critically assessed in the case of Steen basalt, Southern Oregon, USA (Moore et al. 2018). In fact, variation in mineral compositions indicates the balance between magma differentiation process and changing time. Some crucial information related to Continental Flood Basalt genesis is also documented from the Karoo Continental Flood Basalt Province (Heinonen et al. 2013). Some minerals (especially orthopyroxene mineral composition) help to bracket magma evolution at mid-crustal pressure for the Karoo Continental Flood Basalt Province. In the case of the Parana continental magmatic province (at Minas Gerais state, Brazil), elucidation of phase chemistry of constituent minerals (namely, plagioclase, clinopyroxene, subordinate olivine, and opaque oxide phase) of basalts suggests the involvement of at least two parental magmas which were subjected to fractional crystallization (Moraes et al. 2018). In the case of the Kwanza basin in western Angola (related to the Parana Etendeka Flood Basalt province), evolved basalts-to-basaltic andesites, characterized by low TiO_2 (< 2 wt%), have been reported by Marzoli et al. (1999). Based on whole-rock major, trace, and isotope characteristics, these authors have reported tholeiitic and alkaline (and transitional) rock types. The patterns of chemical variation of constituent mineral phases (namely, clinopyroxene olivine plogioclase and spinel) have been deciphered to be commensurate with the nature of host rock types, namely, the tholeiitic basalt, transitional basalts, and alkaline basalt. Crystal size distribution coupled with mineral–chemical data helps to elucidate parental magma composition, magma storage pressure, and emplacement style of mafic dykes and sills from flood basalt provinces. One of such classical studies was made by Macêdo Filho et al. (2019) for the flood basalts of the Parnaiba Basin, Northeastern Brazil.

In the case of the Deccan basalt province, such attempts to understand petrogenetic processes with the help of mineral chemistry were rather rare. Chandrasekharam et al. (2000) worked on the basaltic dyke of the Tapi rift and highlighted unusual abundant clusters of prismatic quenched ferro-enstatite. The authors concluded that these ferro-enstatite crystals have been formed due to the assimilation of shale by the Deccan basaltic magma. They also proposed a liquidus temperature (for the dyke) to be 1220 °C, with crystallization temperature of ferro-enstatite at 1080 °C. Furuyama et al. (2001) worked on an important differentiation center of the Deccan Traps (Pavaghad hill); their studies were based on the chemistry

of constituent minerals such as olivine, clinopyroxene, chrome spinel, and plagioclase. They concluded that olivine and spinel crystallized early, followed by crystallization of clinopyroxene. Plagioclase crystallization took place at the final stage. Based on these mineral–chemical data, it was inferred that basalts of Pavagad hill possibly represent an undepleted lherzolite mantle source located at ~ 85 km depth and 27 kb pressure. Similarly, mineral–chemical data were also used from Pangidi basaltic flows (extension of Deccan basalts) of Andhra Pradesh (Rao et al. 2012) to understand the equilibration temperature of clinopyroxene and coexisting magnetite–ilmenite phases. Furthermore, they believe that lower basaltic flow of that area is represented by higher temperature and a relatively higher amount of glass content as is expected in a differentiating basalt magma. Lightfoot et al. (1990) through their classical work established the stratigraphy of Deccan Trap lavas between Mahabaleswar Ghat and Belgaon areas. These authors have deduced that the bulk rock compositional data (including isotope data), coupled with mineral chemistry, strongly suggest a fractional crystallization model. A similar view of magmatic fractionation history was reported from Deccan Trap lavas occurring near Linga, Eastern Deccan volcanic province (Ganguly et al. 2012). Melluso and Sethna (2011) made a comprehensive review of the available mineral–chemical data for the Deccan Traps of Western India. Those authors have noted wide compositional variations of important constituent phases, such as pyroxene, plagioclase, spinel, ilmenite, and olivine. The range of mineral composition indicates parental magmas with varying degrees of silica saturation and a very similar low-pressure crystallization environment for all the tholeiitic magmas throughout the Deccan.

It is, therefore, evident that mineral–chemistry data for the different parts of Deccan lava flows are available in the literature, with little specific objectives without having detailed effort to understand the petrogenetic evolution. In other words, detailed interpretations of petrogenetic histories of Deccan Trap lavas, utilizing mineral–chemical data alone, are mostly lacking. It is well known that whole-rock geochemical data (major-element, trace-element, and isotopic data) can bring out petrogenetic histories of several continental flood basalt provinces of the world including Deccan basalt (Mahoney 1988). While the whole-rock geochemistry can assess overall petrogenetic aspects satisfactorily in all cases, the use of mineral–chemical data can yield more pin-pointed and incisive data. These mineral–chemical data reveal sound information like density-profiling of the magma, prevailing oxygen fugacity, several magma chamber processes (effect of magma mixing, effervescence characteristics, etc.) and P–T equilibration scenario which are not attainable through whole-rock geochemistry data. Thus, it is apparent that for complete evaluation of petrogenesis,

mineral–chemical data in conjunction with whole-rock geochemistry can be a grand success. However, even mineral–chemical data alone can decipher petrogenetic aspects in vivid details. This approach (use of mineral–chemical data) provides a more effective means to elucidate petrogenesis, since it can critically evaluate some petrogenetic parameters which are beyond the scope of whole-rock geochemical data. Hence, in the present paper, an attempt has been made to unravel a complete picture of petrogenesis embodying mineral chemistry, mineral systematic, textural analysis, geothermobarometry, delineation of density, and oxygen fugacity variation (along lava flow succession). The entire exercise has been worked out on a well-correlated lava flow sequence of the present area of investigation around Khandwa (21° 49′ N:76° 21′ E), Madhya Pradesh which is a part of the Eastern Deccan Volcanic Province (EDVP). The present study has a profound importance since a similar mineral–chemical study can be gainfully undertaken for evaluating the petrogenesis of different flood basalt provinces of the world.

Brief geological background

The Deccan volcanic province (DVP) represents one of the largest continental LIPs on the earth and elucidates one of the world's well-studied continental flood basalt (CFB) provinces that records vast accumulation of laterally extensive basaltic lava flows over extensive continental areas (Self et al. 1997; Sheth 2005; Rajan et al. 2005). The significance of the Deccan volcanic province (DVP) in the global context has been attributed to the vast expanse, enormous volume, and narrow eruption duration almost contemporaneous with the Cretaceous–Paleogene (K–Pg) boundary (~ 66–65 Ma) (Duncan and Pyle 1988; Baksi 1994; Hull et al. 2020). In other words, voluminous outpouring (~ 2×10^6 km^3; Self et al. 1997) of basaltic lavas of DVP had erupted within a very short period. The associated plumbing system of dykes, sills, and layered intrusions represents a spectacular manifestation of earth's internal activities and mantle melting processes (Coffin and Eldholm 1994; Eldholm and Coffin 2000; Ernst and Buchan 2001; Sheth et al. 2009).

The southwestern and western parts of the DVP are geologically well explored in earlier studies (e.g., Mahoney et al. 1982; Mahoney 1988; Cox and Hawkesworth 1984, 1985; Lightfoot and Hawkesworth 1988; Peng et al. 1994; Bondre et al. 2006). It is widely believed that the Satpura–Narmada–Tapi rift system serves as a potential locale for Deccan lava extrusion, especially in the western DVP (Crookshank 1936; West 1958; Bhattacharji et al. 1996; Sheth 2000; Sen and Cohen 1994). Cox and Hawkesworth (1985) and Beane et al. (1986) presented a chemostratigraphy of lavas of the Western Deccan Volcanic Province (WDVP), elucidating details of elemental and isotopic variations.

In comparison to the well-studied WDVP, the quantum of work done in the Eastern Deccan Volcanic Province (EDVP) (where the present area of investigation belongs to) (Fig. 1) is relatively less. In the EDVP, some sporadic sections (including Mandla lobe) have been worked out to understand field geological aspects and geochemical characterization (Crookshank 1936; Alexander and Paul 1977; Yedekar et al. 1996; De 1996; Deshmukh et al. 1996; Pattanayak and Shrivastava 1999; Nair et al. 1996; Peng et al. 1998; Mahoney et al. 2000; Duraiswami et al. 2008; Ganguly et al. 2014; Sengupta and Ray 2007; Kashyap et al. 2010; Sengupta and Ray 2011a, b; Kale et al. 2020; Srinivas et al. 2019). The early study on Eastern Deccan Volcanic Province (EDVP) was initiated by the officers of Geological Survey of India. Those studies mainly include extensive geological mapping at areas located on the northern slope of the Satpura Hills (Crookshank 1936). Later workers attempted to present a systematic classification of EDVP (in disconnected sectors) and correlation of lava flows (Alexander and Paul 1977, Yedekar et al. 1996 and Deshmukh et al. 1996). Lava flow correlation (based on firm physical–volcanological characters) was also proposed almost at the same time (De 1996). Nair et al. (1996) and Kashyap et al. (2010) also attempted to correlate lava flow sequences of EDVP and those of Western Deccan Volcanic Province. In later years, several workers established geochemical finger printing from parts of EDVP using high-precision trace element and isotope data (Pattanayak and Shrivastava 1999; Mahoney et al. 2000; Sengupta and Ray 2011a; Ganguly et al. 2014; Shrivastava et al. 2014). Mineral chemistry of basaltic lava flows (and associated dykes/sills) from several domains of EDVP was also evaluated in an order to bracket the nature of pressure–temperature (P–T) equilibration and prevailing oxygen fugacity of the parent melt (Sen 1980; Sengupta and Ray 2007, 2011b). The study of lava–emplacement geometry (and their bearing on eruption style/geological control) was duly adjudicated in recent years by Kale et al. (2020) and Srinivas et al. (2019). U–Pb zircon age data to constrain earliest eruption time (especially in Malwa plateau area) have recently been given by Eddy et al. (2020) (for a brief description of the studies carried out by these workers, see Supplementary Table S1). However, the available database required to constrain the geochemical and petrological framework of EDVP is still rudimentary.

Field geology

The present area of investigation around Khandwa, Nimur district, Madhya Pradesh (21° 49′ N, 76° 21′ E) records overwhelmingly dominant lava flows with the minor presence
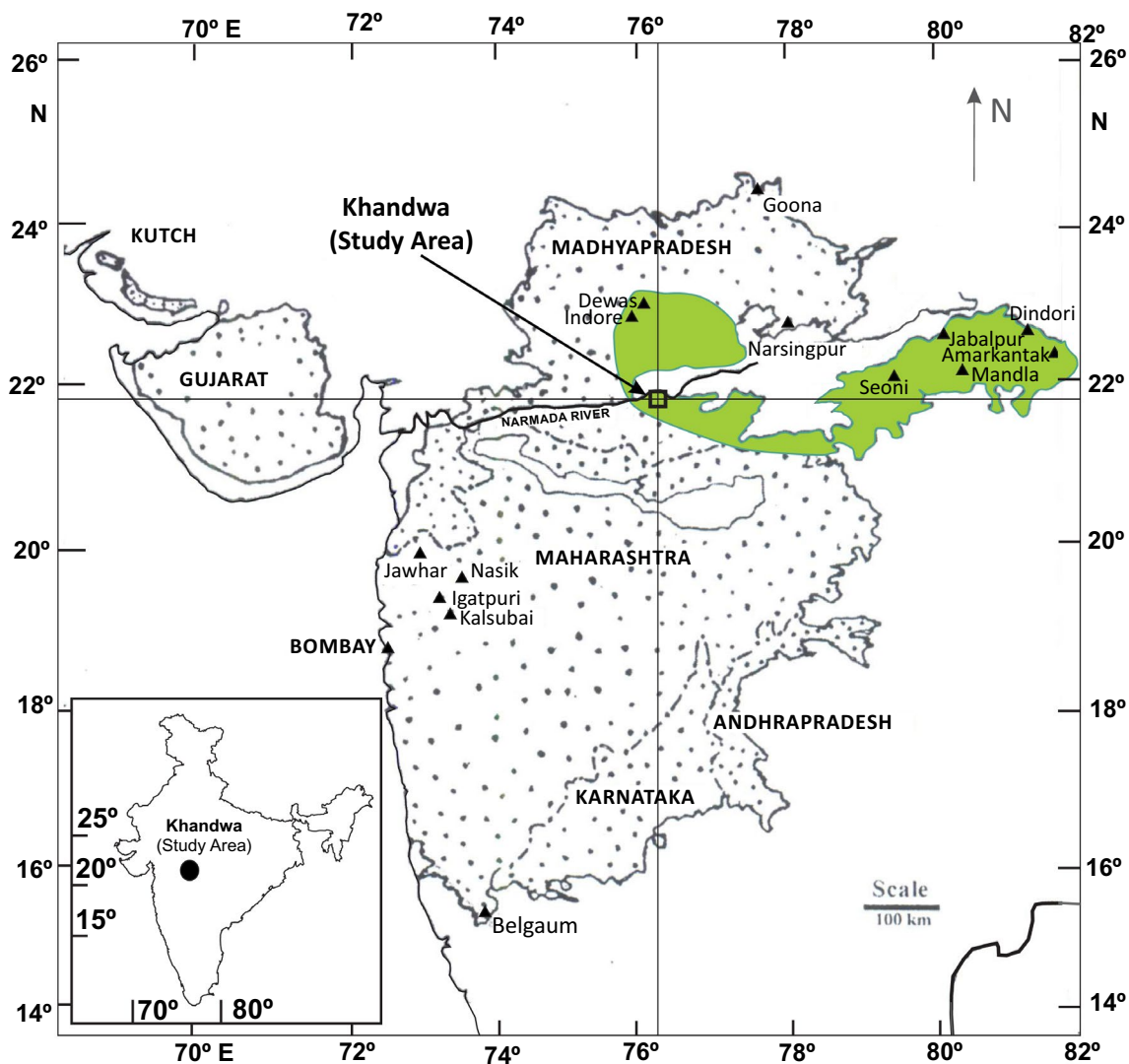
Fig. 1 The distribution of Eastern Deccan volcanic province—EDVP (marked by green)—has been shown within the overall occurrence of Deccan volcanics (stippled). The EDVP domain is after Kashyap et al (2010). The present-study area around Khandwa (unfilled square) falls in the EDVP. Inset map shows location of the study area

of intertrap beds and local alluvium cover (Fig. 2). Extensive field studies were carried out in different sectors of the study area namely, Nagchun, Donwara, Dhanora, Panjra, Jaswari (Fig. 2) which bring out the presence of three distinct lava flows (Flow I, Flow II, and Flow III). All these lava flows were identified using physical volcanological features based on the three-tier classification proposed by earlier workers (De 1972, 1974 and Macêdo Filho et al. 2019). The main premise of such lava flow delineation was the identification of Lower Vesicular Zone (LVZ), Lower colonnade Zone (LCZ), Entablature zone (EZ), Upper colonnade zone (UCZ), and Upper Vesicular Zone (UVZ) based on their development in the fields (Fig. 3a–h). Moreover, the occasional presence of chilled dyke and feeder dyke (both intrusive into Flow II) has been documented. The lava

successions rest over (apparent) cumulate gabbro basement. However, these above-stated zones were not ideally present uniformly throughout the study area and the thickness of such different zones was highly variable. Therefore, lava flow correlation of the study area was based on characteristic structural zones (present in each flows) and topography. In a few places, the presence of local inter trap beds was recorded that helped to correlate lava flows.

Petrography

The petrographic characters of all three flows (namely, Flow I, Flow II, and Flow III) recognized in the study area are zone-specific and monotonous. Some petrographic
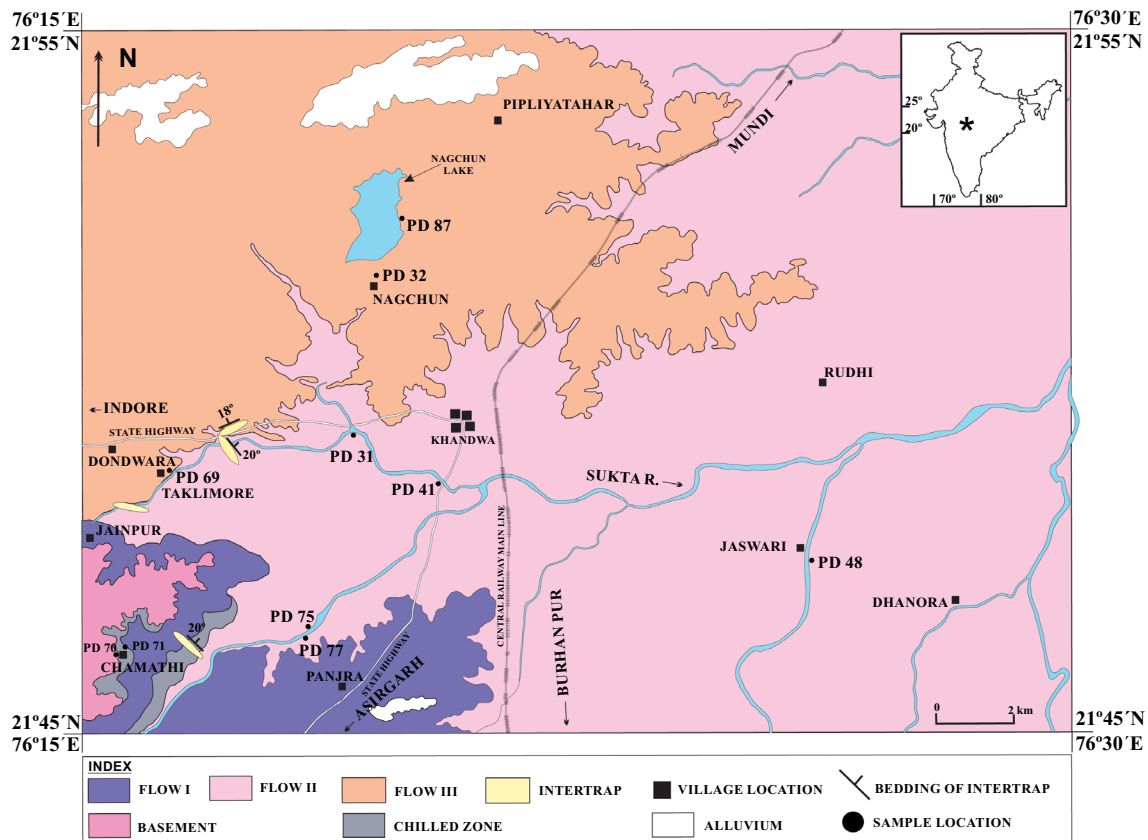
Fig. 2 Geological map of the investigated area around Khandwa (mapped by PD and JR). The intertrap beds in the map mark unconformity-bounded units (UBU) (Lucchi 2019). In the inset, map * denotes the present-study area

variations have, however, been noted for other types, namely, Chilled Dyke, Feeder Dyke, Chilled Zone of lava flows, and Gabbroic basement. Cogent summary of their petrographic characters is given in Supplementary Table S1.1 and supported by Supplementary Fig. S1a-h, Supplementary Figs. S2a–l, S3a–f.

## Mineral chemistry

Olivine

Olivine in investigated lava flows is rather rare (See Supplementary Table S2). Olivine is restricted to UCZ of flow II (found only in PD 41) (Supplementary Fig. S2a). When olivine compositions are plotted in a Mg/ (Fe^{2+} + Mg) vs. Fe^{2+}/(Fe^{2+} + Mg) diagram, they show a slight compositional variation from hyalosiderite to hortonolite (Fig. 4).

Pyroxene

Mineral chemical data of pyroxene were obtained from different representative structural zones and their compositions are given in Supplementary Table S3. The analyzed pyroxene compositions have been considered in an attempt to classify them following IMA nomenclature (Morimoto 1989). As per Q–J relation (where Q = Ca + Mg + Fe and J = 2Na) (expressed in terms of apfu), the analyzed pyroxenes (both phenocryst/micro-phenocryst and groundmass) have been designated as 'quad' pyroxene (Morimoto 1989) (Supplementary Fig. S4a–e). In terms of the Di–Hd–En–Fs quadrilateral (Morimoto 1989), the majority of the plots fall in the augite field, while a few plots also occupy the Pigeonite field (Supplementary Fig. S5a). Pyroxene compositions of flow III are broadly found to fall in the augite field (Supplementary Fig. S5b). For the pyroxene data (corresponding to feeder dyke and chilled dyke), the majority of plots fall in the augite field while a few groundmass pyroxene components also fall in the Pigeonite field (Supplementary Fig. S5c). Chilled zone pyroxene samples show rather restricted composition. They fall in the augite field with a limited compositional spectrum. Only a few samples occupy the pigeonite field (Supplementary Fig. S5d). Pyroxene compositions of basement (gabbro) rocks show a more limited compositional variability and they are restricted to

Fig. 3 Field photographs showing. **a**, **b** Upper Colonnade Zone (UCZ) of flow III, near Nagchun Village; **c** chilled dyke intrusive into flow III, near Panjra village. Long axis of the hammer has been placed perpendicular to the trend of chilled dyke; **d** intertrap (nonclastic type, containing fossils) occurring between flow II and flow III; **e** Upper Vesicular Zone of flow II (near Donwara village); **f** presence of Upper Colonnade Zone (UCZ) and Entablature Zone (EZ) in a single exposure, near Nagchun village. Numerous anastomosing clay veins are present within the EZ; **g** presence of feeder dyke within flow II, near Taklimore village. The long axis of the hammer has been kept perpendicular to the trend of the dyke; **h** coarse-grained Gabbro occurring as basement of lava flows, at Chamathi village
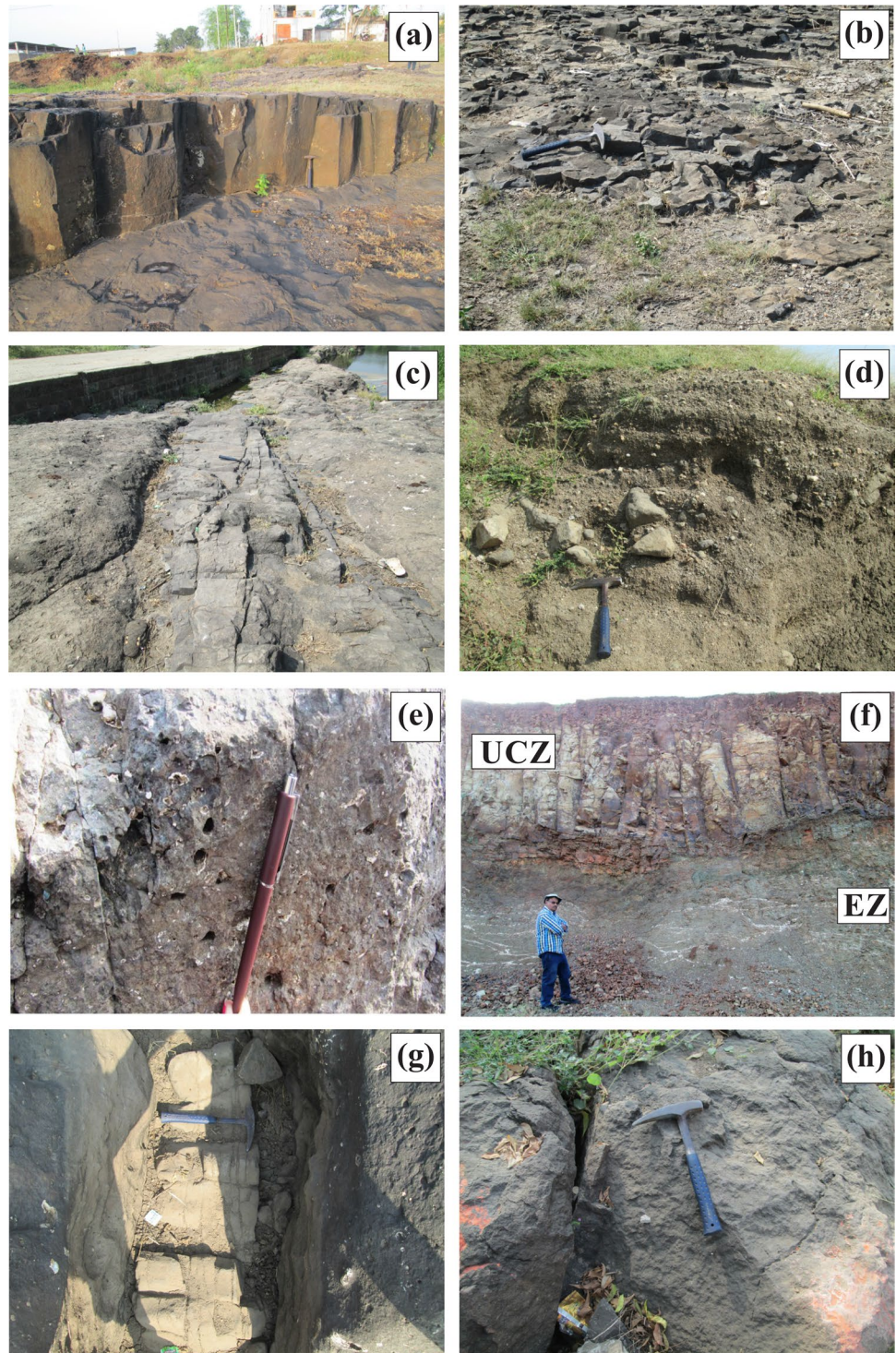

the augite field only; however, one sample plots into the pigeonite field, as well (Supplementary Fig. S5e).

The EPMA data of clinopyroxene involving line scanning (from rim to rim or from core to rim) when plotted on the Di–Hd–En–Fs diagram strongly indicate the presence of compositional variation in different pyroxene grains (Fig. 5a–d). Figure 5a shows a steady rise of Fs content from $\sim Fs_{30}$ to $\sim Fs_{50}$. In Fig. 5b, the upper part of the curve shows a steady rise of Fs content, while the lower part of the curve shows a steep fall of Wo content, which is suggestive of sector zoning. Figure 5c shows Fs enrichment in both wings of the variation curve and Fig. 5d depicts complex sector zoning type.

Fig. 4 Olivine data plots showing compositional spectrum from Hyalosiderite to Hortonolite
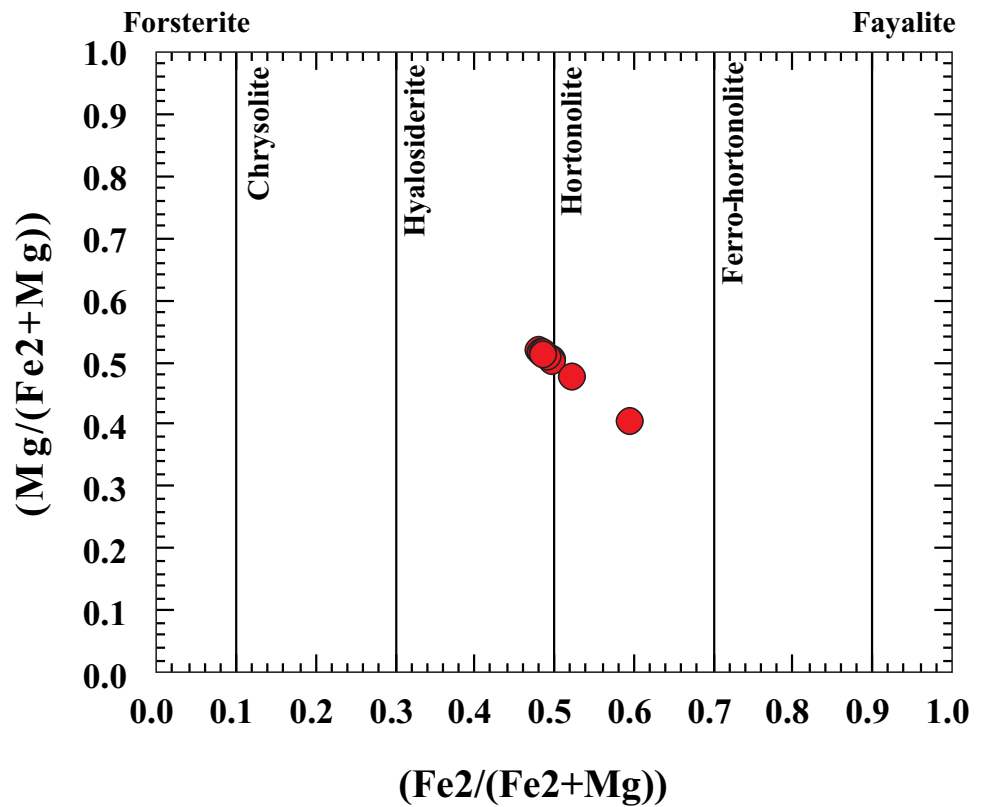
Plagioclase

Plagioclase analyses of the investigated lava flows are given in Supplementary Table S4. Plagioclase phenocrystal compositions of flow II are found to be sufficiently calcic in the Or–Ab–An diagram (Supplementary Fig. S6a) being in the range of bytownite to labradorite. A few groundmass compositions of flow II correspond to andesine. In the case of plagioclase composition of flow III (Supplementary Fig. S6b), a similar behavior of phenocrystal phase and groundmass phase was observed. Plagioclase compositions of both feeder dyke and chilled dyke are plotted in the Or–Ab–An diagram (Supplementary Fig. S6c), which show a broad overlap in the labradorite–andesine range. The plagioclase compositions of the feeder dyke, as expected, show greater tendencies to be clustered in the labradorite field in comparison to the chilled dyke body (Supplementary Fig. S6c). Chilled zone plagioclase composition (which corresponds to parental magma affinity), in an Or–Ab–An diagram, is broadly restricted to the labradorite–bytownite field (showing occasional spill to andesine field) (Supplementary Fig. S6d). Plagioclase compositions from the gabbroic basement in terms of an Or–Ab–An diagram (Supplementary Fig. S6e) show two distinct clusters. The plagioclase phenocrysts display significant compositional variation from rim to rim. The nature of such variation is mostly symmetric (~ An_{58} to ~ An_{80}) with occasional evidence of abrupt change (~ An_{63} to ~ An_{58} through ~ An_{74}) (Fig. 6a–d). The early formed cumulates are distinctly calcic (labradorite), whereas the intercumulas plagioclase is comparatively sodic (andesine). The compositional variation of plagioclase obtained through EPMA studies is in conformity with the cumulus and intercumulus textural evidence in the gabbroic basement (Supplementary Fig. S2 b). This plagioclase compositional variation conforms to the cumulus–intercumulas toggle in a close system magma chamber (Morse 1980).

Opaque minerals (ilmenite and magnetite)

Ilmenite and magnetite analyses of investigated samples are given in Supplementary Tables S5 and S6, respectively. Flow II and flow III (corresponding to UCZ and EZ) have Ti Magnetite samples. Ti magnetite has also been recorded from the chilled zone of flow I and flow II as well as from the chilled dyke and feeder dyke. The basement unit (gabbro) also records Ti magnetite. The other opaque mineral in the investigated samples is found to be ilmenite which has been recorded from UCZ of flow II, feeder dyke, chilled dyke, and chilled zone of flow I and flow II (Supplementary Fig. S2c, f, g, h).
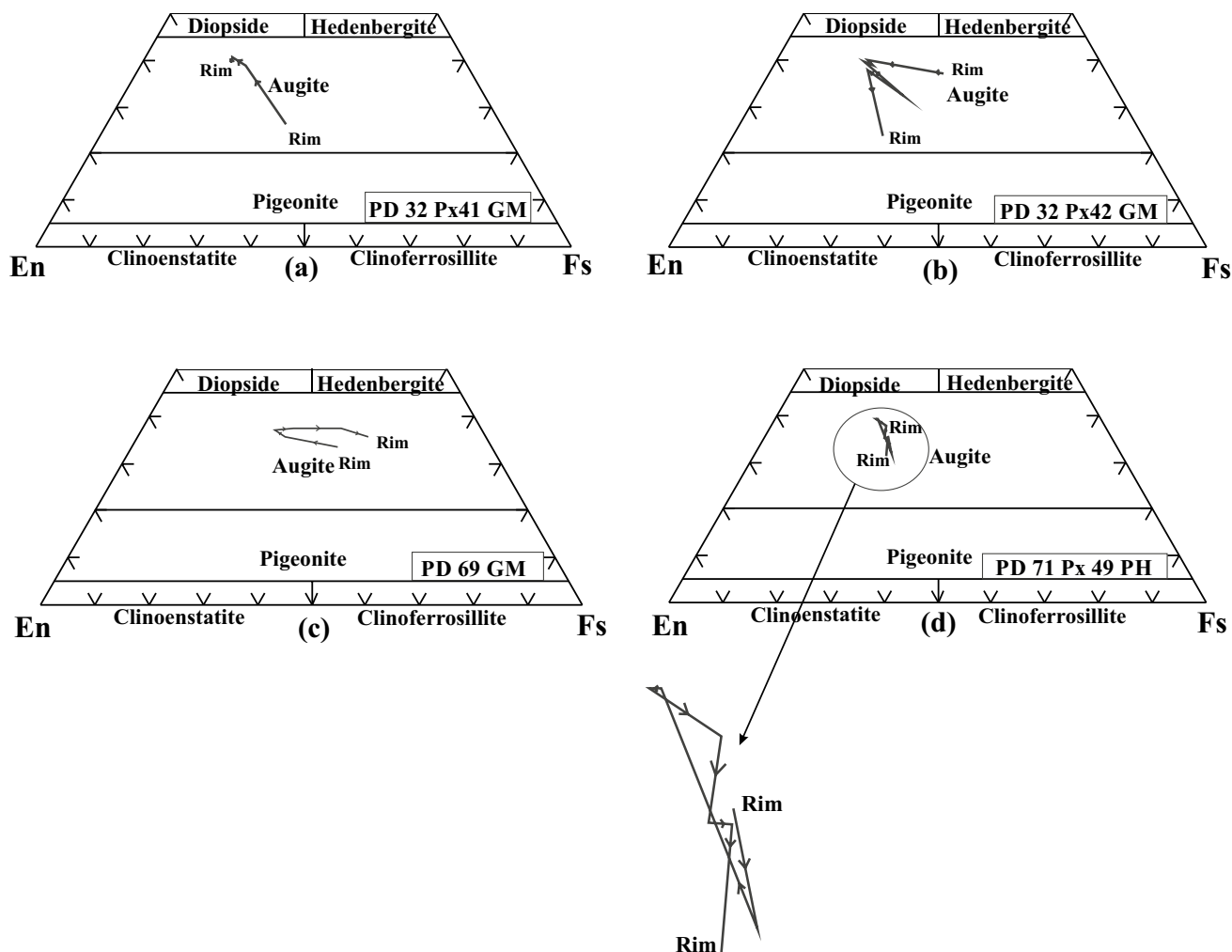
Fig. 5 a–d Styles of pyroxene zoning depicted in terms of Di–Hd–En–Fs quadrilateral (Morimoto 1989). **a**, **b** Flow III Upper Colonnade Zone, **c** Feeder Dyke, intrusive within Flow II, **d** Chilled Zone of Flow I. Px 41, Px 42, and Px 49 refer to individual analysis-points. PD 32, PD 69, and PD 71 denote specimen numbers. PH and GM represent phenocryst and groundmass, respectively

Glass

The isotropic glass of yellow and yellowish-green color has been noticed from flow II and flow III and chilled zones of flow I and flow II. EPMA data of representative glass are given in Supplementary Table S7. It may be noted that the analysis totals are relatively low; but this is a very commonly observed feature, since subsurface charging during EPMA reduces analytical totals. To overcome the low totals, some workers have reported volatile contents ($H_2O \pm CO_2$) by a method known as 'volatiles by difference' (VBD). However, a recent review of literature data (Hughes et al. 2019) shows that this method (VBD) consistently overestimates the volatile contents of glass, and hence, in this present contribution, we did not use this VBD method. Those glass data were referred to in the Total Alkali–Silica diagram (Le Bas et al. 1986) (not

shown), from where it is evident that, in general, the glass has basaltic compositions, while a single sample shows picro-basalt affinity. Representative photomicrographs and BSE images have already been furnished in Supplementary Figs. S1e–g, S2j–l.

Thermometry

Depending on the availability of relevant minerals, we have used the following geothermometers which are: (1) Pyroxene geothermometer (after Lindsley 1983), (2) glass thermometer (after Helz and Thornber 1987; Montierth et al. 1995 and Putirka 2008), and (3) magnetite–ilmenite geothermometer (Powell and Powell 1977). The thermometric data obtained by different methods as stated above are given in Table 1.
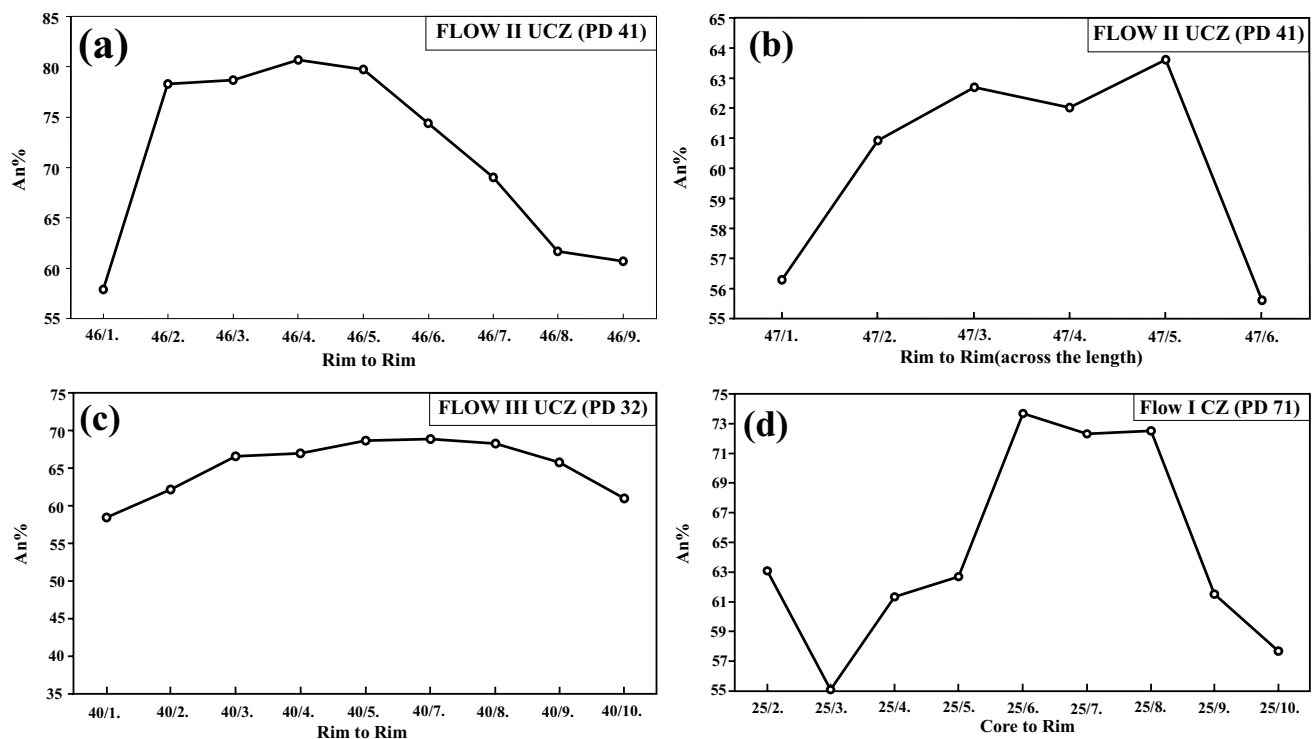
Fig. 6 **a–d** Variation pattern of An% in zoned plagioclase in several structural zones corresponding to different flows. PD 41, PD 32, and PD 71 denote sample numbers. *UCZ* upper colonnade zone, *EZ* entablature zone, *CZ* chilled zone

Pyroxene thermometry

Determining temperature using pyroxene composition is an effective and rewarding method (Lindsley 1983). The raw apfu data of pyroxene composition, of course, need to be recalculated in terms of Wo, En, and Fs end-members. The pyroxene thermometry method (Lindsley 1983) is essentially a graphical one where the pyroxene composition of a particular rock needs to be plotted with respect to experimentally obtained thermal contours. The output data faithfully portray the thermal equilibration of the host rock containing pyroxene. In this view, pyroxene thermometry (Lindsley 1983) has been attempted for the investigated lava flows and associated chilled zone, feeder dyke, chilled dyke, and the gabbro basement. The projected pyroxene compositions in such contour diagrams are shown in Supplementary Fig. S7a-e and the corresponding data are given in Table 1. From the data in Table 1, it is evident that thermometric values deduced for flow II range from 1050 to 1130 °C, whereas thermometric values for flow III range from 1080 to 1105 °C. The chilled dyke (occurring within flow II) gives an equilibration temperature of 1052 °C, whereas the feeder dyke also exposed in flow II gives a temperature of 1015 °C. The chilled zone corresponding to flow II and flow I shows a limited or restricted temperature range of 1013–1108 °C. The basement (gabbroic unit) gives a relatively lower

thermometric value (1020 °C). In general, the pyroxene thermometric data yield a relatively restricted temperature range (1015–1130 °C) where the higher bound corresponds to early formed phenocryst phases.

Glass thermometry

A glass or liquid thermometer provides a useful means for understanding the equilibration temperature of volcanic rock (Putirka 2008). A simple method involving glass thermometer was initially postulated by Helz and Thornber (1987), where wt% MgO in the glass (~ liquid composition) was given consideration. Subsequently, the Helz and Thornber (1987) thermometer was revised by Montierth et al. (1995). It was suggested by Putirka (2008) that, although those above-mentioned thermometers are simple enough, they work remarkably well. However, Putirka (2008) noted a systematic error in the thermometer proposed by Helz and Thornber (1987) and subsequently removed the error proposing a new model, which is:

$$T(°C) = 26.3 \, MgO^{(Liq)} + 994.4°C.$$

In the present study, glass thermometry was attempted using the methods of Helz and Thornber (1987) and Montierth et al. (1995) with the updated thermometer advocated

Table 1 Thermometry data of pyroxene, glass, and oxide phases

Flow name	Sample location	Sample no	Structural zone	Wo' (range)	En' (range)	Fs' (range)	Deduced temperature (°C)[a]	Deduced temperature (°C) (Putrika 2008)	(Helz and Thornber 1987)	(Montierth et al. 1995)	X_{ulv}	X_{ilm}	Deduced temperature (°C)
				Pyroxene thermometry (Lindsley, 1983)				**Glass thermometry**			**Oxide thermometry (Powell and Powell 1977)**		
Flow II	21° 49′ 18.5″ N 76° 19′ 11.0″ E	PD 31	UCZ	37.05 10.85	54.47 38.54	46.8 11.91	1130	1365	1297	1336	0.257	0.967	632
Flow II	21° 48′ 30.1″ N 76° 20′ 31.0″ E	PD 41	UCZ	38.3 34.85	45.31 43.08	23.83 16.72	1050	–	–	–	0.776	0.862	1303
Flow II	21° 47′ 27.8″ N 76° 26′ 01.9″ E	PD 48	UCZ	38.15 24.95	48.39 28.39	46.66 16.33	1075	1355	1290	1328	–	–	–
Flow III	21° 51′ 35.6″ N 76° 19′ 33.8″ E	PD 32	UCZ	38.3 23.3	49.63 31.59	36.12 14.7	1105	1421	1340	1385	–	–	–
Flow III	21° 52′ 12.39″ N 76° 19′ 46.04″ E	PD 87	EZ	38.5 37.75	48.88 47.8	14.3 13.37	1080	1264	1220	1248	–	–	–
Flow II	21° 48′ 44.30″ N 76° 16′ 19.02″ E	PD 69	FD	39.75 22.85	51.08 22	50.25 15.78	1015	1387	1314	1356	0.779	0.934	1093
Flow II	21° 46′ 36.94″ N 76° 18′ 30.68″ E	PD 75	CD	38.35 23.3	48.67 31.81	34.84 18.88	1053	1162	1142	1159	0.774	0.913	1156
Flow I	21° 46′ 09.98″ N 76° 15′ 40.34″ E	PD 71	CZ	36.55 13.95	54.45 37.55	34.75 18.5	1108	1203	1174	1195	0.651	0.902	1045
Flow II	21° 46′ 21.28″ N 76° 18′ 29.49″ E	PD 77	CZ	39.05 11.95	47.65 34.05	48.8 17.16	1013	1321	1263	1297	0.804	0.879	1306
	21° 46′ 06.66″ N 76° 15′ 29.45″ E	PD 70	B	38.6 13.86	45.86 23.32	45.13 25.14	1020	–	–	–	–	–	–

UCZ upper colonnade zone, *EZ* entablature zone, *FD* feeder dyke, *CD* chilled dyke, *CZ* chilled zone, *B* basement

[a]Represents mean deduced temperature (Lindsley 1983)

by Putirka (2008) (Table 1). All these methods yield a quite consistent and fairly well-defined range of liquidus temperatures. Glass thermometry after Putrika (2008) indicates that, for the UCZ (of all the flows), the temperature varies from 1355 to 1421 °C. For EZ, the temperature is seemingly low (1264 °C). The glass thermometry obtained for the feeder dyke is 1387 °C; in the case of the chilled dyke, the temperature is relatively lower (1162 °C). Glass thermometry data for the CZ (chilled zone) of flow II are 1321 °C, while in case of CZ (chilled zone) of flow I, it is found to be relatively lower (1203 °C). However, the Putirka (2008) method slightly overestimates the temperature.

Magnetite–ilmenite geothermometry

In this study, we have used the independent Iron–Titanium oxide geothermometer given by Powell and Powell (1977) which is based on experimental data of Buddington and Lindsley (1964). We have calculated X_{ulv} and X_{ilm} following the Powell and Powell (1977) method and those data are presented in Table 1. We next calculated K_D, ln K_D, and temperature in °C following Eq. 3 of Powell and Powell (1977). The deduced temperatures (Table 1) show a range from 632 to 1306 °C. Except for two samples of Flow II and one sample of the chilled zone, the pyroxene thermometry data are broadly similar to that obtained from magnetite–ilmenite thermometry. The oxide thermometry suggests that the opaque phases (mostly surficial) equilibrated for a relatively broader temperature range.

Tracking crystallization history through quantitative modeling

Quantitative modeling of the crystallization history of basaltic magma has often been attempted through software involving an algorithm that helps petrologists to understand the mineral-melt equilibrium model and quantification of physical parameters such as density, viscosity, and oxygen fugacity. In the present study, we attempted such quantitative modeling with Petrolog 3 software (Danyushevsky and Plechov 2011). This software offers a model- independent algorithm, which enables workers to deal with a large number of mineral-melt equilibria models and several physical characters of the melt (such as density and viscosity). The Petrolog-3 offers a unique opportunity to the community of igneous petrologists to work with a very user-friendly interface for computer simulation related to the crystallization process. This particular software enables us to understand the appearance (or disappearance) of several constituent mineral phases during magmatic evolution. This is particularly helpful to decipher the paragenetic appearance of constituent phases (both phenocryst and groundmass) in a basaltic magma (Morse 1980; Philpotts and Ague 2009).

The output data obtained using Petrolog 3 software are given in Table. 2. To validate these data, petrographic and textural evidence for each of the specimen has been thoroughly examined. It is evident that, while the Petrolog 3 output serves as an excellent tool for the initial estimation of several parameters, it gives the insight to understand several magmatic processes only when coupled with detailed petrographic observations. For each sample, detailed output from Petrolog 3 and relevant textural support is furnished in Supplementary Table S8. Initial magma temperature was ascertained with glass thermometric data (Putirka 2008).

It is evident that the parent magma suffered both equilibrium and fractional crystallization. As for example in the majority of the cases, olivine crystallized initially in the magma chamber, and subsequently, it started reacting with the ambient liquid. This would lead to the complete disappearance of olivine. As a result of olivine and liquid reaction during equilibrium crystallization, augitic clinopyroxene will be the stable phase. The magma, in turn, might have started the separation of relevant phases now represented by the phenocrysts (fractional crystallization). The parent magma, therefore, represents a combination of both, equilibrium and fractional crystallization, an expected behavior close to reality (Morse 1980). From Petrolog 3 software, liquidus temperatures of different mineral phases can be obtained. These data (with relevant petrographic support) were duly assessed to understand the groundmass temperature. Groundmass opaque (temperature) was given due consideration to have an idea of melt solidification. The surficial magma eruption temperature could be constrained well with the help of groundmass minerals. Again within the groundmass component tiny pyroxene, slender thin plagioclase and surficial opaque minerals have been documented on the basis of petrographic analyses. Our calculation indicates that after reaching the surface, magma started crystallizing at ~ 1250 °C (revealed by plagioclase thermometry using plagioclase groundmass composition, see Supplementary Table S4) which was closely followed by tiny clinopyroxene groundmass (~ 1215 °C) (pyroxene thermometry Lindsley 1983). These two minerals were next joined by opaque minerals (~ 1150 °C) (Powell and Powell 1977). Of course, there is small-to-moderate degree of overlap pertaining to crystallization temperatures of these three phases, which is very usual. In general, textural data support that opaque minerals in the groundmass were crystallized at the last and that has been supported by our thermometric calculations as well, as stated above. Tables 1 and 2 indicate that clinopyroxene started crystallizing (as phenocryst phase) at ~ 1150–1200 °C. The crystallization of clinopyroxene continued up to ~ 800 °C as depicted by pyroxene thermometry (Lindsley 1983) of the groundmass components (see Supplementary Table S3). Similarly, plagioclase phenocrysts started crystallizing at ~ 1100 °C (see Table 2

Table 2 Various parameters related to crystallization history of the lava flows using Petrolog-3 software

Serial no.	Sample no.	Structural zone	First formed crystal (temperature, °C)	Prevalent O$_2$ fugacity	Magma density (gm/cc)	Crystallization phase I (temperature, °C)	Crystallization phase II (temperature, °C)	Crystallization phase III (temperature, °C)	Crystallization phase IV (temperature, °C)	Glass thermometry(°C)[a]
1	PD 31	FLOW II UCZ	OL (1340)	− 6.90	2.81	CPX (1187)	MT (1169)	PLAG (1029)	ILM (760)	1365
2	PD 48	FLOW II UCZ	OL (1347)	− 6.80	2.91	MT(1212)	CPX (1204)	ILM (1098)	PLAG (963)	1355
3	PD 32	FLOW III UCZ	OL (1378)	− 6.50	2.78	CPX (1226)	MT (1187)	ILM (933)	PLAG (921)	1421
4	PD 87	FLOW III EZ	ILM (1327)	− 10.7	2.71	OL (1268)	MT (1121)	PLAG (1106)	CPX (1087)	1264
5	PD 69	FEEDER DYKE	OL (1395)	− 6.4	2.76	CPX (1225)	MT (1175)	ILM (1117)	PLAG (937)	1387
6	PD 75	CHILLED DYKE	ILM (1327)	− 7.0	3.28	MT (1327)	OL (1239)	PLAG (1123)	CPX (1065)	1162
7	PD 71	FLOW I CHILLED ZONE	OL (1254)	− 7.7	2.89	MT (1203)	CPX (1134)	ILM (1027)	PLAG (895)	1203
8	PD 77	FLOW II CHILLED ZONE	OL (1327)	− 7.0	2.84	CPX (1208)	MT (1190)	ILM (963)	PLAG (891)	1321

For sample nos. PD 48, PD 32, PD 69, and PD 77, Petrolog-3 data slightly overestimate pyroxene liquidus temperature compared to pyroxene thermometry (Lindsley 1983) (Table 1); accuracy of Lindsley (1983) method is 20–30 °C within the experimentally calibrated range

OL olivine, *CPX* clinopyroxene, *MT* magnetite, *ILM* ilmenite, *PLAG* plagioclase, *UCZ* upper Colonnade zone, *EZ* entablature zone

[a]Glass thermometry data (Putrika 2008) have been incorporated from Table 1 for comparison of liquidus temperatures of several phases with reference to parent melt temperature

Petrolog- 3 data). This thermometric value remains almost the same for the groundmass plagioclase. Careful scrutiny of Table 1 reveals that ~ 632 °C is the ultimate magmatic crystallization temperature (opaque thermometry method, Powell and Powell 1977). Another interesting character (that has been revealed through the Petrolog-3 program) is the variation of magma density with the onset of crystallization. The density in the evolving magma ranges from 2.71 gm/cc to 3.28 gm/cc. Likewise, oxygen fugacity (during the magmatic evolution) changes from—10.7 log (fO$_2$) to—6.4 log (fO$_2$). The reason for such variations is discussed in the subsequent sections.

Discussion

Nature of crystallization in parental magma

Continental Flood Basalt (CFB) Provinces cover large areas within the Earth's surface and the compositions of erupted basalts are essentially controlled by (1) characteristics of primary magma and (2) modification imposed upon them during their journey before eruption onto the Earth's surface (Wilson 1989). Often, the parental magmas reflect their source characteristics (Wilkinson and Binns 1977) and mantle lithology at different water saturation levels (Prestvik and Goles 1985). The relation between silica and iron-rich primary magma-composition for many CFB provinces has been attributed to subduction modified mantle (Wilson 1989). In general, the CFB provinces are marked by the characteristic presence of plagioclase ± clinopyroxene ± olivine phenocrysts (Cox 1980), which suggests low-pressure crystal fractionation (Wilson 1989). According to Morse (1980), the crystallization of basaltic magma is neither a manifestation of only equilibrium crystallization or fractional crystallization. Rather, in nature, it is often a combination of both equilibrium and fractional crystallization. Textural analysis often serves as a useful tool to understand complex petrogenetic processes.

Plagioclase composition from the present study also portrays the evolutionary history of the magma, at least during the time after the plagioclase touches the liquidus. It has been shown in an earlier section that rim-to-rim compositional variation in plagioclase phenocryst is either symmetric or kinked. This suggests fractional crystallization of the plagioclase from the parent magma (Fig. 6a–d) occasionally being controlled by water pressure fluctuation (Philpotts and Ague 2009) (Supplementary Fig. S8a–e). The fractionating behavior of the parental magma is more effectively adjudicated in terms of pyroxene phenocryst chemistry where, besides pyroxene separation, a collage of varieties of zoning characteristics are present. These are simple type, sector type, and complex sector types (Fig. 5a–d), which are indicative of complex interplay of changing physico-chemical processes in several micro- and macro-domains in the magma chamber during pyroxene separation. Thus, in the present case, fractional crystallization, by and large, plays a major role in the evolution of the magma (in other words, equilibrium crystallization was a subsidiary mechanism).

Glass chemistry and nature of fractionation vis-a-vis petrographic evidence

We used analyzed glass composition (adopting normalization procedure given by Hughes et al. 2019) as a useful proxy to understand magma behavior (Putirka 2008). Projection of glass composition in terms of the plagioclase–olivine–quartz normative diagram (Dilek et al. 1999) (Fig. 7) gives an idea of the ambient pressure of the parent magma during crystallization and quenching. The data corresponding to different zones (Fig. 7) show some scatter. The chilled dyke (intrusive into flow II) represents olivine-rich pristine chemistry that corresponds to a sufficiently high-pressure equilibration within the magma chamber (pressure > 15 kb). The data corresponding to (1) Feeder dyke (Feeder dyke within flow II), (2) UCZ of flow II, (3) UCZ of flow III, and (4) chilled zone of flow II represent a relatively higher pressure (~ 15 kb) which corresponds to roughly 45 km depth within the magma chamber. On the contrary, the glass composition corresponding to the chilled zone of flow I and EZ of flow III is located closer to 1 atm line (Fig. 7). Thus there is a barometric variation for different zones of several lava flows. This implies that different isotropic glasses noticed within the lava successions are not merely rapidly quenched products corresponding to the normal surficial condition. In other words, there is clear evidence of the distinct presence of glasses formed at higher pressure which were subsequently thrown out and embedded in the surficially formed groundmass and retained their 'higher magnitude pressure ambience'.

Evaluation of the controlling tectonic setting

Evaluation of the tectonic setting of basaltic rocks with the help of discrimination diagrams is a conventional practice by many geologists. The pioneer worker who initiated this approach was Pearce et al. (1976, 1996) where the basic connotation was to decipher the tectonic setting of basalts of unknown affinity based on the geochemistry of modern-day basalts of varied tectonic settings. In other words, the main tenet of this approach is 'present is the key to the past' (Law of uniformitarianism). The tectonic setting of the investigated basalts was evaluated using parent magma compositions obtained through glass chemistry of different samples (see Supplementary Table S7). One of the useful major-element diagrams to discriminate tectonic settings is

Fig. 7 Plots of glass compositions for different representative samples in terms of normative plagioclase–olivine–quartz plot. Explanation of abbreviation: *UCZ* upper colonnade zone, *EZ* entablature zone, *FD* feeder dyke, *CD* chilled dyke, *CZ* chilled zone, *B* basement (Gabbro). Equilibration pressure lines (1 atm, 10 kb, and 15 kb) have been incorporated from Dilek et al. (1999). PD 31, PD 48, etc. denote specimen numbers. Data plotting far below 15 kb equilibration line (as, for example, PD 75) represent high-pressure formation; during sudden eruption, they form 'fossilized glass', which may be later included in opaque minerals. For details, see text
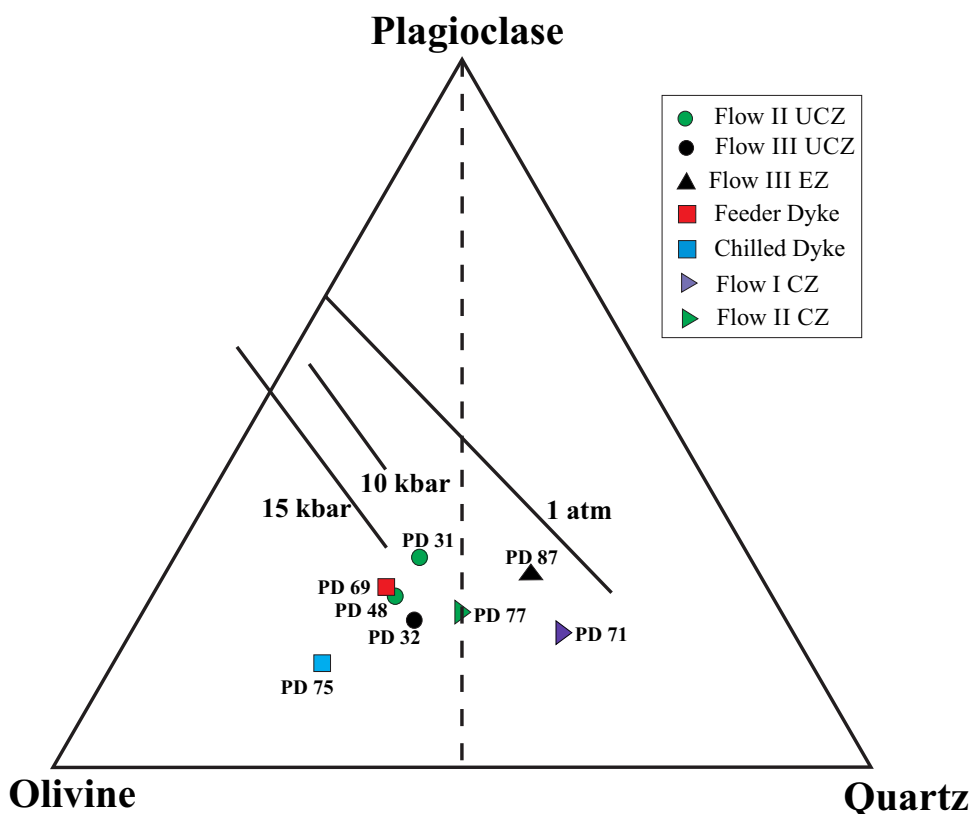
on the basis of the TiO_2(wt%)–K_2O(wt%)–P_2O_5(wt%) diagram (Pearce et al. 1975). All the present data plots fall within field B (continental) (Fig. 8). The mineral chemistry of clinopyroxene (belonging to host basaltic rock) is a good indicator to unravel tectonic settings (Leterrier et al. 1982). Clinopyroxene compositions of the basaltic rocks of the study area when referred to the Ti (apfu) vs. Ca (apfu) diagram after Leterrier et al. (1982) (Fig. 9) clearly suggest the 'non-orogenic' nature. Therefore, tectonic discrimination diagrams involving major-element chemistry of the constituent glass and mineral chemistry (especially clinopyroxene mineral chemistry) are a clear indication of having a 'continental' tectonic setting. This is in tune with the studies made by Mahoney (1988), Wilson (1989), Coffin and Eldholm (1992), Peng et al. (1994), and Melluso and Sethna (2011).

Viewing magma chamber processes

To view magma chamber conditions, magma chamber processes, and modification of the parent magma through several evolutionary stages, Petrolog software (Petrolog 2 and Petrolog 3) was originally designed by Ghiorso et al. (2002). This software can effectively demonstrate processes like partial melting, fractional crystallization, and reverse fractional crystallization using a complex algorithm (Danyushevsky and Plechov 2011). Noting the effectiveness of this software, in this paper, we attempt to

model the details of magma crystallization procedures, magma chamber processes, and the appearance of liquidus temperature of several constituent phases. The Petrolog 3 program was also used to model the crystallization behavior of several phases including liquidus phase estimation, oxygen fugacity calculation, and progressive change-over of density parameters. Interestingly, for almost all zones involving several flows, olivine was the first formed mineral (according to Petrolog 3) inside of the magma chamber. As modal olivine is seldom found, we infer that, in almost all cases, olivine was totally reacted upon (with the ambient liquid) to give rise to clinopyroxene. The opaque phases (magnetite and ilmenite) that appeared at the very early stage of magmatic crystallization could not have survived as a phenocrystal phase because of prevalent low oxygen fugacity during their formative stage in the magma chamber. In other words, the initially formed oxide phases (magnetite and ilmenite) virtually vanished or became unstable immediately after their formation. Magnetite and ilmenite, which are almost ubiquitous as groundmass phases of the investigated lavas, formed at high oxygen fugacity, after lava eruption and stabilization at the surface. Figure 10 is a schematic lithology, showing different lava flows of the study area and several structural zones therein. The accompanying panel of the same figure (Fig. 10) depicts the variation of oxygen fugacity of ambient magma from bottom to top as well as density

Fig. 8 Plot of different representative glass compositions (parent melt) in wt% TiO_2–K_2O–P_2O_5 diagram (after Pearce et al. 1975). All data plots fall within field B (continental). PD 71, PD 77, etc. denote sample numbers
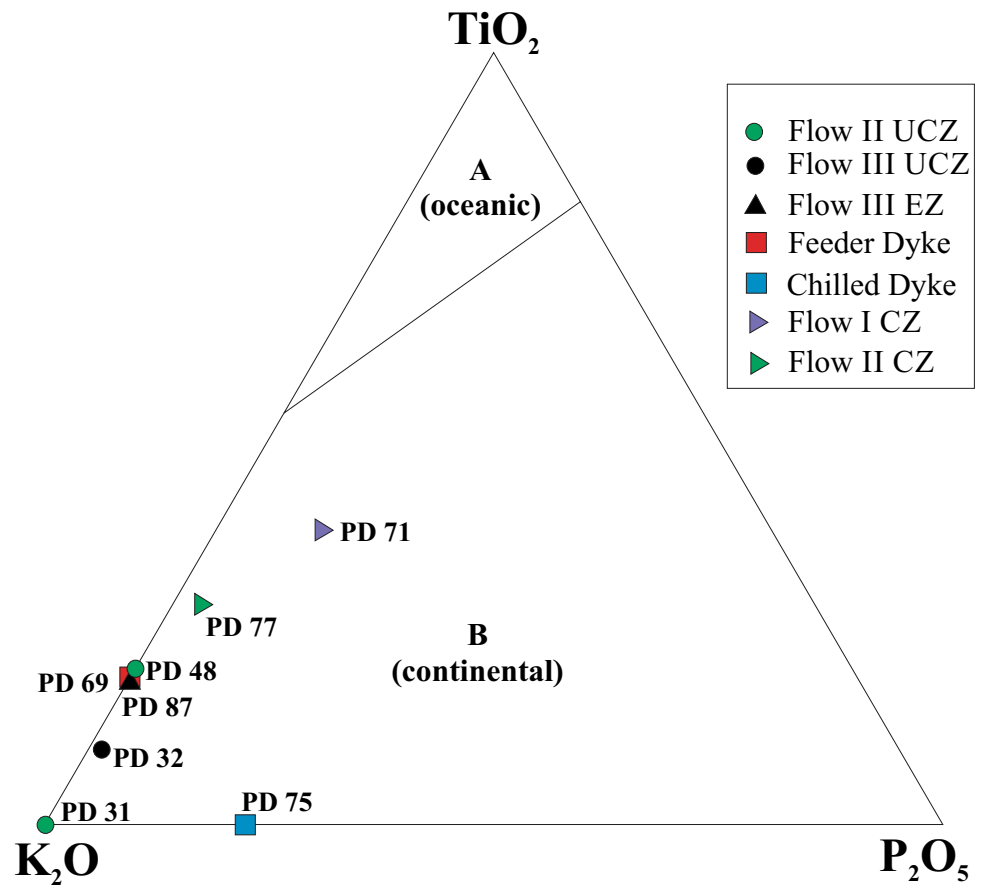
variation. The oxygen fugacity from bottom to top shows a slight oscillatory pattern. The –log(fO2) changes from 7.7 (chilled zone of flow I) to ~ 7 (chilled zone of flow II). The oxygen fugacity oscillatory pattern may be ascribed to heating and reduction during magma ascent. Density of magma is one of the important controlling factors on the eruptibility of magmas. It has been found that there is a strong correlation between magma density and corresponding volume of the lava flow (Hartley and Maclennan 2018). Over about 85% of the total volume of the volcanic eruption lies close to a density-minimum that corresponds to the composition of basaltic magma at the arrival of plagioclase at the liquidus. This type of density- minimum magma is buoyant enough which facilitates the magma to erupt in a profuse volume. The use of a simple numerical model has shown that eruption of magma with relatively higher density is assisted by the generation of overpressure in the magma chamber (Hartley and Maclennan 2018). In the present case, it is, therefore, evident that the density-minimum of the magma (~ 2.70–2.80 gm/cc) produced more voluminous and abundant lava flow (mostly Flow III and less commonly Flow II) and the feeder dyke. On the other hand, magma corresponding to the Chilled zones of lava flows and Chilled dyke (and locally some

portion of Flow II) bear higher densities (~ 2.90 gm/cc), and they have restricted field occurrences (they correspond to localized domains of magma–chamber–overpressure). Anderson and Wright (1972) documented (contrary to popular belief) that, during the onset of magma eruption, it effervesces and suffers a reducing environment because of (1) loss of H_2O, (2) loss of SO_2, and (3) magma mixing. Furthermore, there is a conspicuous correlation between oxygen fugacity and temperature variation. In support of their contention, Anderson and Wright (1972) referred to the case of Tristan de Cunha lavas. This lava underwent strong reduction during eruption because of loss of volatile materials, particularly SO_2 (Anderson 1968). Magma effervescence during ascent is found to be a definite cause of accelerated crystallization of microphenocryst, rise in temperature, and decrease in oxidation state. We, therefore, conclude that the Deccan volcanism (as revealed in the present study) shows a complex interplay of repeated pulses of magma ascent, fluctuation of the crystallization condition, effervescence, and local magma mixing. The petrogenetic aspects of the flood basalt provinces (~ LIP) in different parts of the world have been attempted by various workers in recent years (Heinonen et al 2013; Moore et al 2018; Moraes et al 2018) using high-precision

Fig. 9 Ti (apfu) vs. Ca (apfu) plots for the investigated clinopyroxene in the tectonic discrimination diagram suggested by Leterrier et al. (1982). Almost all samples occupy field D (non-orogenic basalts) [apfu: atoms per formula unit]
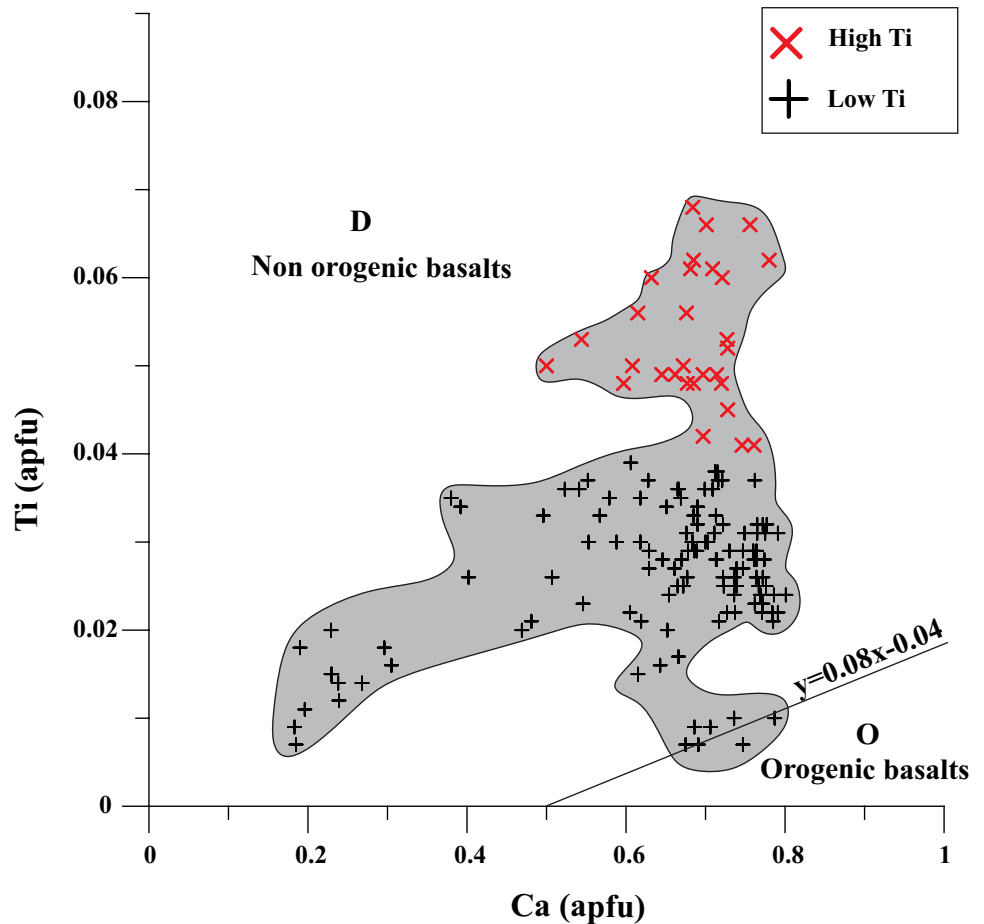
whole-rock geochemical data. For the Deccan volcanic province of the Indian shield, similar attempts (to understand petrogenesis) is in vogue since almost the middle of the last century (Alexander and Paul 1977; Yedekar et al 1996; Peng et al 1998; Pattanayak and Shrivastava 1999; Mahoney et al 2000). Recent studies by several workers (Sengupta and Ray 2011a, b; Vanderkluysen et al. 2011; Ganguly et al 2014; Patel et al. 2020) using whole-rock geochemical data have substantially improved our knowledge related to Deccan petrogenesis. However, our present study highlights the importance of mineral–chemical study of the constituent phases (from different units like several lava flows, dykes, chilled zones, etc.) to assess the petrogenetic evolution of the Deccan Traps. In other words, it has been shown that, based on sound field data and petrographic analyses, mineral chemistry of constituent phases can independently provide a good insight into the magma chamber processes. Significant information about the appearance of several liquidus phases, range of crystallization temperature, nature of oxygen fugacity, density variation in the ambient magma, relevant petrological consequences (like development of typical textures, relative dominance of lava flows, etc.), and controlling tectonic

milieu were clearly brought out from our present study. We, therefore, contemplate that similar mineral– chemical studies (with or without conjunction of whole-rock chemical data) can be gainfully undertaken for other flood basalt provinces of the world.

Conclusions

The present study attempts to elucidate petrogenetic aspects (from parts of Eastern Deccan Flood Basalt Province) through comprehensive mineral–chemical studies. The Deccan trap volcanic province (which is a part of Continental Flood Basalts) covers large areas within the Earth's surface and is essentially controlled by characteristics of the primary magma or any subsequent modification (from the magma chamber en route) before their eruption onto the Earth's surface. In the present investigation, the constituent phases, namely, plagioclase and pyroxene (both phenocryst and groundmass), display significant compositional variation marked by several zoned geometry, suggesting the effect of fractional crystallization in the parent magma. It is evident that glass compositions (belonging to different
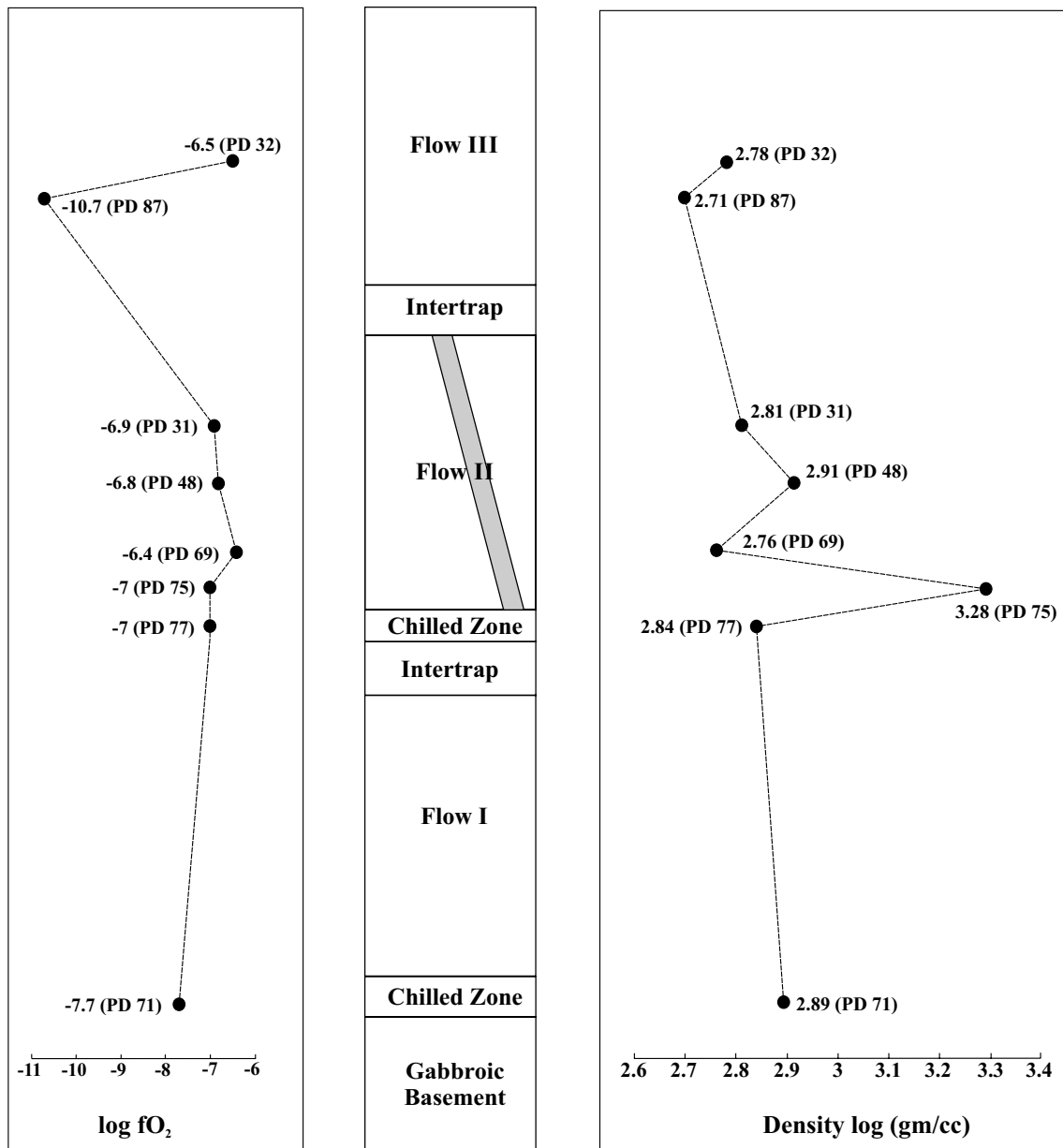
Fig. 10 Panel diagram showing a schematic disposition of several lava flows, chilled zone, feeder dyke, intertrap, etc. The left-hand side panel diagram shows the variation of log fO_2 while the right-hand side panel diagram shows density variation (gm/cc) [PD 71, PD 77, etc. denote sample numbers]

structural zones of the investigated lava sequences) suggest varied ambient pressures which range from > 15 kb (fossilized glass) to a surficial pressure regime. Glass compositions corresponding to such contrasting ambiance have been corroborated by textural studies (Supplementary Fig. S1e, f, and g). The glass compositions were effectively used to evaluate the tectonic setting of the relevant discrimination diagrams. Use of the TiO_2 (wt%)–K_2O (wt%)–P_2O_5 (wt%) diagram (Pearce et al. 1975) favors a 'Continental' setting. Mineral chemistry is a good assessor of tectonic setting (Leterrier et al. 1982) and clinopyroxene composition in the

present case indicates a 'non-orogenic' continental setting. Petrolog 3 software was used to model the magma crystallization procedure, internal magma chamber processes, the appearance of liquidus temperature of several phases, and switch over of oxygen fugacity and density parameters. A critical assessment of Petrolog 3 output data was made in conjunction with detailed petrographic analyses to arrive at a sound conclusion pertaining to the crystallization condition of the parent magma. It has been inferred that initially found olivine reacted with the ambient liquid in the magma chamber in an equilibrium crystallization milieu. Early formed

opaque phases also disappeared due to prevalent low oxygen fugacity. We demonstrate that Deccan volcanism (as revealed in the present study) shows a complex interplay of repeated pulses of magma ascent, fluctuating crystallization conditions, effervescence, and local-scale magma mixing, evaluated on the basis of comprehensive mineral chemistry. A similar study (taking mineral chemistry as the main assessor) may be effectively extended to other Continental Flood Basalts of different parts of the world.

References

Alexander PO, Paul DK (1977) Geochemistry and strontium isotopic composition of basalts from the eastern Deccan volcanic province, India. Mineral Mag 41:165–171

Anderson AT (1968) The oxygen fugacity of alkaline basalt and related magmas, Tristan da Cunha. Am J Sci 266:704–727

Anderson AT, Wright TL (1972) Phenocrysts and glass inclusions and their bearing on oxidation and mixing of basaltic magmas, Kilauea volcano. Hawaii Am Mineral J Earth Planet Mater 57:188–216

Baksi AK (1994) Geochronological studies on whole-rock basalts, Deccan Traps, India: evaluation of the timing of volcanism relative to the KT boundary. Earth Planet Sci Lett 121:43–56

Beane JE, Turner CA, Hooper PR et al (1986) Stratigraphy, composition and form of the Deccan basalts, Western Ghats, India. Bull Volcanol 48:61–83

Bhattacharji S, Chatterjee N, Wampler JM (1996) Zones of Narmada-Tapi rift reactivation and Deccan volcanism: geochronological and geochemical evidence. Deccan Basalts Gondwana Geol Soc Nagpur 329–340

Bondre NR, Hart WK, Sheth HC (2006) Geology and geochemistry of the Sangamner mafic dike swarm, western Deccan volcanic province, India: implications for regional stratigraphy. J Geol 114:155–170

Buddington AF, Lindsley DH (1964) Iron-titanium oxide minerals and synthetic equivalents. J Petrol 5:310–357

Chandrasekharam D, Vaselli O, Sheth HC, Keshav S (2000) Petrogenetic significance of ferro-enstatite orthopyroxene in basaltic dikes from the Tapi rift, Deccan flood basalt province, India. Earth Planet Sci Lett 179:469–476

Coffin MF, Eldholm O (1994) Large igneous provinces: crustal structure, dimensions, and external consequences. Rev Geophys 32:1–36

Coffin MF, Eldholm O (1992) Volcanism and continental break-up: a global compilation of large igneous provinces. Geol Soc Lond Spec Publ 68:17–30

Cox KG (1980) A model for flood basalt vulcanism. J Petrol 21:629–650

Cox KG, Hawkesworth CJ (1985) Geochemical stratigraphy of the Deccan Traps at Mahabaleshwar, Western Ghats, India, with implications for open system magmatic processes. J Petrol 26:355–377

Cox KG, Hawkesworth CJ (1984) Relative contribution of crust and mantle to flood basalt magmatism, Mahabaleshwar area,

Deccan Traps. Philos Trans R Soc London Ser A, Math Phys Sci 310:627–641

Crookshank H (1936) Geology of the Northern slopes of the Satpuras between Morand and Sher Rivers-Mem. Geol Sur India 66:

Danyushevsky LV, Plechov P (2011) Petrolog 3: Integrated software for modeling crystallization processes. Geochemistry, Geophys Geosystems, p 12

De A (1996) Entablature structure in Deccan Trap flows: its nature and probable mode of origin. Gond Geol Mag 2:439–447

De A (1974) Short and long distance correlation of Deccan Trap lava flows. Bull Geol Min Met Soc India 47:50

De A (1972) Structural features of the Deccan Trap tholeiitic basalt flows of southern Kutch. In: Proc. Indian Sci. Congress 56 th Session, Part. p 180

Deshmukh SS, Sano T, Fujii T et al (1996) Chemical stratigraphy and geochemistry of the basalt flows from the central and eastern parts of the Deccan Volcanic Province of India. Gondwana Geol Mag Spec 2:145–170

Dilek Y, Thy P, Hacker B, Grundvig S (1999) Structure and petrology of Tauride ophiolites and mafic dike intrusions (Turkey): Implications for the Neotethyan ocean. Geol Soc Am Bull 111:1192–1216

Duncan RA, Pyle DG (1988) Rapid eruption of the Deccan flood basalts at the Cretaceous/Tertiary boundary. Nature 333:841–843

Duraiswami RA, Bondre NR, Managave S (2008) Morphology of rubbly pahoehoe (simple) flows from the Deccan Volcanic Province: implications for style of emplacement. J Volcanol Geotherm Res 177:822–836

Eddy MP, Schoene B, Samperton KM et al (2020) U-Pb zircon age constraints on the earliest eruptions of the Deccan Large Igneous Province, Malwa Plateau. India Earth Planet Sci Lett 540:116249

Eldholm O, Coffin MF (2000) Large igneous provinces and plate tectonics. Geophys Monogr Geophys UNION 121:309–326

Ernst RE, Buchan KL (2001) Mantle plumes: their identification through time. Geological Society of America

Furuyama K, Hari KR, Santosh M (2001) Crystallization history of primitive Deccan basalt from Pavagadh Hill, Gujarat, western India. Gondwana Res 4:427–436

Ganguly S, Ray J, Koeberl C et al (2012) Mineral chemistry of lava flows from Linga area of the Eastern Deccan Volcanic Province, India. J Earth Syst Sci 121:91–108

Ganguly S, Ray J, Koeberl C et al (2014) Geochemistry and petrogenesis of lava flows around Linga, Chhindwara area in the Eastern Deccan Volcanic Province (EDVP), India. J Asian Earth Sci 91:174–193

Ghiorso MS, Hirschmann MM, Reiners PW, Kress VC (2002) The pMELTS: a revision of MELTS for improved calculation of phase relations and major element partitioning related to partial melting of the mantle to 3 GPa. Geochem Geophys Geosyst 3:1–35

Hartley M, Maclennan J (2018) Magmatic densities control erupted volumes in Icelandic volcanic systems. Front Earth Sci 6:29

Heinonen JS, Luttinen AV, Riley TR, Michallik RM (2013) Mixed pyroxenite–peridotite sources for mafic and ultramafic dikes from the Antarctic segment of the Karoo continental flood basalt province. Lithos 177:366–380

Helz RT, Thornber CR (1987) Geothermometry of Kilauea Iki lava lake. Hawaii Bull Volcanol 49:651–668

Hughes EC, Buse B, Kearns SL et al (2019) Low analytical totals in EPMA of hydrous silicate glass due to sub-surface charging: Obtaining accurate volatiles by difference. Chem Geol 505:48–56

Hull PM, Bornemann A, Penman DE, et al (2020) On impact and volcanism across the Cretaceous-Paleogene boundary. Science (80-) 367:266–272

Kale VS, Dole G, Shandilya P, Pande K (2020) Stratigraphy and correlations in Deccan Volcanic Province, India: Quo vadis? GSA Bulletin 132:588–607

Kashyap M, Shrivastava JP, Kumar R (2010) Occurrence of small scale inflated pahoehoe lava flows in the Mandla lobe of the eastern Deccan volcanic province. Curr Sci 72–76

Krishnamurthy P (2019) Carbonatites of India. J Geol Soc India 94:117–138

Le Bas MJ, Maitre RWLE, Streckeisen A et al (1986) A chemical classification of volcanic rocks based on the total alkali-silica diagram. J Petrol 27:745–750

Leterrier J, Maury RC, Thonon P et al (1982) Clinopyroxene composition as a method of identification of the magmatic affinities of paleo-volcanic series. Earth Planet Sci Lett 59:139–154

Lightfoot P, Hawkesworth C (1988) Origin of Deccan Trap lavas: evidence from combined trace element and Sr-, Nd-and Pb-isotope studies. Earth Planet Sci Lett 91:89–104

Lightfoot PC, Hawkesworth CJ, Devey CW et al (1990) Source and differentiation of Deccan Trap lavas: implications of geochemical and mineral chemical variations. J Petrol 31:1165–1200

Lindsley DH (1983) Pyroxene thermometry. Am Mineral 68:477–493

Lucchi F (2019) On the use of unconformities in volcanic stratigraphy and mapping: Insights from the Aeolian Islands (southern Italy). J Volcanol Geotherm Res 385:3–26

Macêdo Filho AA, Archanjo CJ, de Hollanda MHBM, Negri FA (2019) Mineral chemistry and crystal size distributions of mafic dikes and sills on the eastern border of the Parnaíba Basin, NE Brazil. J Volcanol Geotherm Res 377:69–80

Mahoney J, Macdougall JD, Lugmair GW et al (1982) Origin of the Deccan Trap flows at Mahabaleshwar inferred from Nd and Sr isotopic and chemical evidence. Earth Planet Sci Lett 60:47–60

Mahoney JJ (1988) Continental flood basalts. Petrol Struct Geol 3:151–194

Mahoney JJ, Sheth HC, Chandrasekharam D, Peng ZX (2000) Geochemistry of flood basalts of the Toranmal section, northern Deccan Traps, India: implications for regional Deccan stratigraphy. J Petrol 41:1099–1120

Marzoli A, Melluso L, Morra V et al (1999) Geochronology and petrology of Cretaceous basaltic magmatism in the Kwanza basin (western Angola), and relationships with the Paraná-Etendeka continental flood basalt province. J Geodyn 28:341–356

Melluso L, Sethna SF (2011) Mineral compositions in the Deccan igneous rocks of India: an overview. In: Topics in igneous petrology. Springer, pp 135–159

Mjle BAS, Maitre RWLE, Streckeisen A et al (1986) A chemical classification of volcanic rocks based on the total alkali-silica diagram. J Petrol 27:745–750

Montierth C, Johnston AD, Cashman KV (1995) An empirical glass-composition-based geothermometer for Mauna Loa lavas. Washingt DC Am Geophys Union Geophys Monogr Ser 92:207–217

Moore NE, Grunder AL, Bohrson WA (2018) The three-stage petrochemical evolution of the Steens Basalt (southeast Oregon, USA) compared to large igneous provinces and layered mafic intrusions. Geosphere 14:2505–2532

Moraes LC, Seer HJ, Marques LS (2018) Geology, geochemistry and petrology of basalts from Parana Continental Magmatic Province in the Araguari, Uberlandia, Uberaba and Sacramento regions, Minas Gerais state Brazil. Braz J Geol 48:221

Morimoto N (1989) Nomenclature of pyroxenes. Can Mineral 27:143–156

Morse SA (1980) Basalts and phase diagrams: an introduction to the quantitative use of phase diagrams in igneous petrology. Springer-Verlag, New York, p 493

Nair KKK, Chatterjee AK, Sano T (1996) Stratigraphy and geochemistry of the Deccan basalts along Toranmal section, western Satpura region. Gondwana Geol Mag 2:23–48

Palmer DAS, Williams-Jones AE (1996) Genesis of the carbonatite-hosted fluorite deposit at Amba Dongar, India; evidence from fluid

inclusions, stability isotopes, and whole rock-mineral geochemistry. Econ Geol 91:934–950

Patel V, Sheth H, Cucciniello C et al (2020) Geochemistry of deccan tholeiite flows and dykes of elephanta island: insights into the stratigraphy and structure of the panvel flexure zone, Western Indian Rifted Margin. Geosciences 10:118

Pattanayak SK, Shrivastava JP (1999) Petrography and major-oxide geochemistry of basalts from the Eastern Deccan Volcanic Province, India. Mem Soc India, pp 233–270

Pearce JA (1976) Statistical analysis of major element patterns in basalts. J Petrol 17:15–43

Pearce JA (1996) A user's guide to basalt discrimination diagrams Trace Elem geochemistry Volcan rocks. Appl Massive Sulfide Explor Geol Assoc Canada Short Course Notes 12:79–113

Pearce TH, Gorman BE, Birkett TC (1975) The TiO_2–K_2O–P_2O_5 diagram: a method of discriminating between oceanic and non-oceanic basalts. Earth Planet Sci Lett 24:419–426

Peng ZX, Mahoney J, Hooper P et al (1994) A role for lower continental crust in flood basalt genesis? Isotopic and incompatible element study of the lower six formations of the western Deccan Traps. Geochim Cosmochim Acta 58:267–288

Peng ZX, Mahoney JJ, Hooper PR et al (1998) Basalts of the northeastern Deccan Traps, India: isotopic and elemental geochemistry and relation to southwestern Deccan stratigraphy. J Geophys Res Solid Earth 103:29843–29865

Philpotts A, Ague J (2009) Principles of igneous and metamorphic petrology. Cambridge University Press, Cambridge, p 667

Powell R, Powell M (1977) Geothermometry and oxygen barometry using coexisting iron-titanium oxides: a reappraisal. Mineral Mag 41:257–263

Prestvik T, Goles GG (1985) Comments on petrogeneses and the tectonic setting of Columbia River basalts. Earth Planet Sci Lett 72:65–73

Putirka KD (2008) Thermometers and barometers for volcanic systems. Rev Mineral Geochem 69:61–120

Rajan S, Tiwary A, Pandey D (2005) The Deccan volcanic province: thoughts about its genesis. www mantleplumes org/Deccan2 html

Rao PVN, Swaroop PC, Karimulla S (2012) Mineral chemistry of Pangidi basalt flows from Andhra Pradesh. J Earth Syst Sci 121:525–536

Ray JS, Shukla PN (2004) Trace element geochemistry of Amba Dongar carbonatite complex, India: Evidence for fractional crystallization and silicate-carbonate melt immiscibility. J Earth Syst Sci 113:519–531

Self S, Thordarson T, Keszthelyi L (1997) Emplacement of continental flood basalt lava flows. Geophys Monogr Geophys UNION 100:381–410

Sen G (1980) Mineralogical variations in the Delakhari sill, Deccan trap intrusion, central India. Contrib Mineral Petrol 75:71–78

Sen G, Cohen TH (1994) Deccan intrusion, crustal extension, doming and the size of the Deccan-Reunion plume head. Volcanism Wiley Eastern, New Delhi, pp 201–216

Sengupta P, Ray J (2007) Mineral chemistry of basaltic lava flows from Narsingpur–Harrai–Amarwara–Lakhnadon areas of Eastern Deccan, Central India. Igneous Petrol 21st century Perspect, pp 37–72

Sengupta P, Ray J (2011a) Petrogenesis of Flood Basalts of the Narsingpur–Harrai–Amarwara–Lakhnadon Section of Eastern Deccan Province, India. In: Topics in igneous petrology. Springer, pp 191–238

Sengupta P, Ray J (2011b) Petrology of the mafic sill of Narshingpur-Lakhnadon section, Eastern Deccan volcanic province. J Geol Soc India 77:309–327

Sheth HC (2005) Were the Deccan flood basalts derived in part from ancient oceanic crust within the Indian continental lithosphere? Gondwana Res 8:109–127

Sheth HC (2000) The timing of crustal extension, diking, and eruption of the Deccan flood basalts. Int Geol Rev 42:1007–1016

Sheth HC, Ray JS, Ray R et al (2009) Geology and geochemistry of Pachmarhi dykes and sills, Satpura Gondwana Basin, central India: problems of dyke-sill-flow correlations in the Deccan Traps. Contrib Mineral Petrol 158:357

Shrivastava JP, Mahoney JJ, Kashyap MR (2014) Trace elemental and Nd-Sr-Pb isotopic compositional variation in 37 lava flows of the Mandla lobe and their chemical relation to the western Deccan stratigraphic succession, India. Mineral Petrol 108:801–817

Srinivas K, Kishore PP, Rao DVS (2019) The geological site characterisation of the Mandla region, Eastern Deccan Volcanic Province. Central India J Earth Syst Sci 128:139

Srivastava RK (1997) Petrology, geochemistry and genesis of rift-related carbonatites of Ambadungar, India. Mineral Petrol 61:47–66

Vanderkluysen L, Mahoney JJ, Hooper PR et al (2011) The feeder system of the Deccan Traps (India): insights from dike geochemistry. J Petrol 52:315–343

West WD (1958) The petrography and petrogenesis of forty eight flows of Deccan Traps penetrated by borings in western India. Trans Indian Natl Inst Sci 4:1–56

Wilkinson JFG, Binns RA (1977) Relatively iron-rich lherzolite xenoliths of the Cr-diopside suite: a guide to the primary nature of anorogenic tholeiitic andesite magmas. Contrib Miner Petrol 65:199–212

Wilson M (1989) Igneous petrogenesis. Unwin Hyman, London, p 466

Yedekar DB, Aramaki S, Fujii T, Sano T (1996) Geochemical signature and stratigraphy of the Chhindwara–Jabalpur–Seoni–Mandla sector of the Eastern Deccan Volcanic Province and problems of its correlation. Gondwana Geol Mag Spec 2:49–68